Energy Proceedings
Vol 36, 2023
ISSN 2004-2965

Photo-enhanced Catalytic DRM on Ni@SiO$_2$ with High Resistance to Carbon Deposition

Jinrui Zhang[1,2], Tianlong Yang[1,3], Qiong Rao[1,2], Yang Li[1,2], Zhongrui Gai[1,3], Ying Pan[1*]

1 Institute of Engineering and Thermophysics, Chinese Academy of Sciences, Beijing, 100190, China

2 University of Chinese Academy of Sciences, Beijing, 100190, China

3 International Research Center for Renewable Energy & State Key Laboratory of Multiphase Flow in Power Engineering, Xi'an Jiaotong University, Xi'an, 710049, China

(*Corresponding Author: panying@iet.cn)

ABSTRACT

Methane and carbon dioxide are major greenhouse gases contributor. CO_2 dry reforming of methane (DRM) for syngas production is a promising approach to reducing global CO_2 emission and extensive utilization of natural gas. However, the reported catalysts endured rapid deactivation due to severe carbon deposition at high temperature. Here, CO_2 reduction by CH_4 on hexagonal nano-nickel flakes wrapped by porous SiO_2 (Ni@SiO$_2$) catalysts driven by thermal and solar light are tested. High resistance to carbon deposition and reactive activity are demonstrated under focused solar light. Furthermore, the mechanism of light-enhanced reaction reactivity is investigated by Infrared spectroscopy and the activation effect of light is depicted. The light-driven DRM provides a promising method for renewable solar energy conversion and CO_2 emission reduction due to the excellent activity and durability.

Keywords: syngas, photocatalytic DRM, CO_2 emission reduction, resistance to carbon deposition

1. INTRODUCTION

The worldwide researchers have devoted to reduce the emission of greenhouse gases for years, which was mainly consisted of carbon dioxide and methane. The dry reforming of methane (DRM) emerged as a promising method for CO_2 and CH_4 utilization, as described in (1) [1,2].

$$CH_4 + CO_2 \rightleftharpoons 2\text{CO} + 2H_2, \Delta H_{298}^{\theta} = 247kJ/mol \quad (1)$$

However, the side reactions, mainly the reverse water-gas shift (RWGS) (2) and the methane cracking reaction (3), lead to carbon deposition and lower H_2/CO ratio[3].

$$CO_2 + H_2 \rightleftharpoons \text{CO} + H_2O, \Delta H_{298}^{\theta} = 41kJ/mol \quad (2)$$

$$CH_4 \rightleftharpoons C_{(S)} + 2H_2, \Delta H_{298}^{\theta} = 75kJ/mol \quad (3)$$

The highly endothermic DRM reaction always requires high temperature (>700 ℃) for promoting reaction proceeding, with a large amount of energy input[4]. Therefore, concentrated solar energy is a promising energy source for supplying the heat requirement in DRM, realizing clean solar energy conversion and storage[5].

The reported thermal catalysts for DRM always contain noble metals to enhance the reactivity. However, the carbon deposition and metal sintering under high temperature always led to the deactivation of catalysts[6,7]. As the high cost and insufficient reserve of precious metals, Ni-based catalyst has been explored as alternatives due to its considerable activity and abundance[8,9]. Nevertheless, nickel meets more severe issue of carbon deposition, which mainly caused by the thermodynamically favorable CH_4 decomposition and CO disproportionation[10,11]. Therefore, it is attractive to develop Ni-based catalyst with carbon resistance, excellent reactivity, and high durability.

To inhibit the sintering of Ni and reducing the heat dissipation of sample, core-shell structure consisted of Ni and inert shell can be considered for metal separation and heat insulation. Among virous support as CeO_2, TiO_2, Al_2O_3, SiO_2, and ZrO_2, SiO_2 attracts widespread attention due to its inertness, excellent stability, and controlled surface properties[12,13]. And researchers have widely studied Ni-based catalysts over various silica support for thermocatalytic DRM, such as mesoporous SBA-15, MCM-41, and KIT-6[14–17]. However, few studies about

This is a paper for the 9th Applied Energy Symposium: Low Carbon Cities and Urban Energy Systems (CUE2023), Sep. 2-7, 2023, Matsue & Tokyo, Japan.

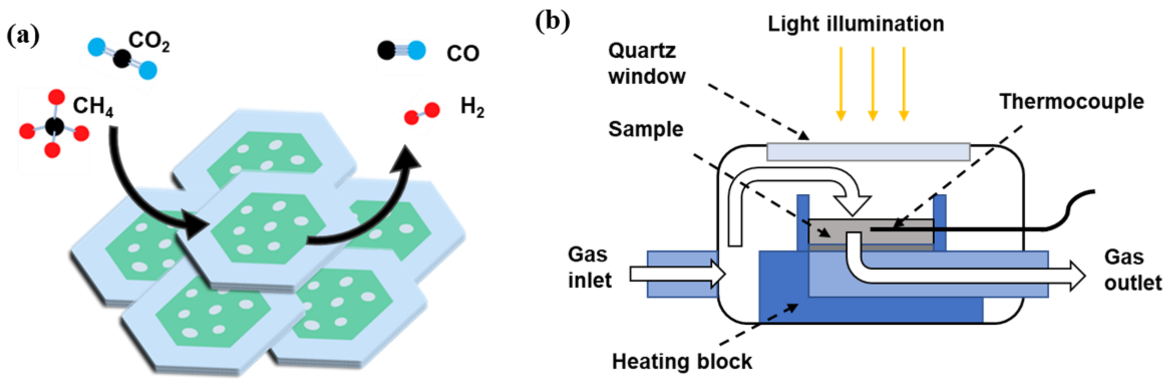

Fig. 1 (a) The depict of the reaction process. (b) Schematic representation of the reactor

modified SiO_2 supported Ni catalyst for light-driven DRM reaction have been reported. Cai et al. designed a core-shell structured Ni@SiO_2 hexagonal nanosheet with heat insulation and infrared shielding effects of SiO_2 shell for light-driven RWGS reaction.[18]. The Ni@SiO_2 catalyst showed significant enhancement in conversion rate and carbon resistance under focus solar illumination. Nevertheless, this catalyst has not been further explored in methane dry reforming process.

2. MATERIAL AND METHODS

2.1 Sample synthesis

Ni@SiO_2 was synthesized through a hydrothermal method. $Ni(NO_3)_2 \cdot 6H_2O$ and Polyvinyl Pyrrolidone (PVP) were dissolved in ultrapure water under magnetic stirring. Then $NH_3 \cdot H_2O$ solution (28%) was added to adjust the pH to 8. After 1 h stirring, the solution was sealed into autoclave and heated at 150 °C for 36 h. Then the precipitate was washed with water and collected by centrifugation, and dispersed in ethanol water. The SiO_2 shell was then coated through a sol-gel method, adding $NH_3 \cdot H_2O$ solution (28%) and Tetraethyl orthosilicate into the solution with vigorous stirring for 1 h. Then the solid was collected by centrifugation and dried at 110 °C overnight. The dried particles were calcined at 400 °C for 4 h with heating rate at 10 °C per minute. The schematic diagram of the reaction process was shown in Fig. 1a.

2.2 Material characterization

The scanning electron microscope (SEM) images was obtained by FE-SEM Zeiss MERLIN compact. Transmission electron microscope (TEM) images was obtained by field emission transmission electron microscopy (JEM-F200) operated at 200 kV acceleration voltage. UV-VIS-NIR adsorption data was captured by UV–vis-Nir diffuse reflectance absorption spectrum (Agilent Cary 7000). Catalyst crystal phase test was carried on by X-Ray Diffractometer (Bruker D8 Focus).

2.3 Experimental set-up

The tests of reactive performance were carried by a commercial photoreactor (Fig. 1b) with a quartz window. In each test, 15 mg of catalyst was added into the sample cup of a diameter of 7 mm. A thermocouple was placed under the irradiation surface to directly measure the actual reaction temperature under focused solar light. The light source was supplied by a 300 W Xenon lamp (MC-PF300C) equipped with a convex lens of 120 mm focal length. The reaction temperature was controlled at 400, 450 and 500 °C, which were corresponding to the light intensity of 7.3, 8.8 and 10.6 W/cm^2, respectively.

In a catalytic test, the sample was first purged with Ar (30 mL/min) for 30 min and activated with H_2 (10 mL/min) at 500 °C for 5 min. After another purge for 30 min, the sample was heated under Ar atmosphere (30 mL/min) to the settled temperature by electrical heating elements or light. Then CH_4 (5 mL/min) and CO_2 (5 mL/min) were introduced into the reactor, and the outlet gas was collected with gas bags for each 5 min. A GC (Agilent 8890) was used for the products analysis, which equipped with TCD and FID detectors.

A Bruker INVENIO-S FTIR spectrometer was used for the *in-situ* diffuse reflectance Infrared Fourier transform spectroscopy (DRIFTS) test with the same reactor equipped with a specialized 4-window cap. The gas flow was the same as ex-situ part, and the reaction temperature was settled at 450 °C for both dark and light reaction.

2.4 Calculation

For data processing, the conversion rates of the reactants were calculated according to the following equations,

$$F_{out} = F_{in,Ar} / X_{out,Ar} \qquad (4)$$

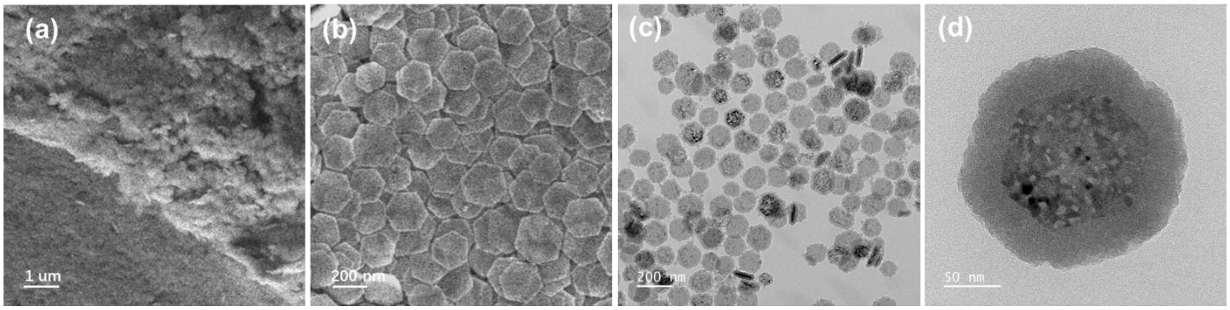

Fig. 2 (a) (b) Scanning electron microscope (SEM) images and (c) (d) Transmission electron microscope (TEM) images of as-prepared $Ni@SiO_2$ sample.

$$F_{out,i} = X_{out,i} \cdot F_{out} \quad (5)$$
$$X_{CH_4} = (F_{in,CH_4} - F_{out,CH_4})/F_{in,CH_4} \quad (6)$$
$$X_{CO_2} = (F_{in,CO_2} - F_{out,CO_2})/F_{in,CO_2} \quad (7)$$

where F is the flow rate of the gases, X is the conversion of reactant, i means the specific gas species, and subscript in and out are corresponding to the inlet and outlet gases. Further, the consuming and producing rate of gases were deduced as following:

$$r_{CH_4} = (F_{in,CH_4} \cdot X_{CH_4} \cdot P_r)/(m \cdot R \cdot T_{out}) \quad (8)$$
$$r_{CO_2} = (F_{in,CO_2} \cdot X_{CO_2} \cdot P_r)/(m \cdot R \cdot T_{out}) \quad (9)$$
$$r_{H_2} = (F_{out,H_2} \cdot P_r)/(m \cdot R \cdot T_{out}) \quad (10)$$
$$r_{CO} = (F_{out,CO} \cdot P_r)/(m \cdot R \cdot T_{out}) \quad (11)$$

here r is the conversion or production rate of the reactants, m represents the mass of sample, P_r is the reaction pressure (1 atm), T_{out} is room temperature (273.15 K), and R is the gas constant at room temperature.

For the data of TGA (Thermogravimetric Analysis) test, the weight percentage of oxidized $NiO@SiO_2$ was recorded as X_1, and that of the reduced $Ni@SiO_2$ as X_2. Thereby, the weight percentage of $Ni@SiO_2$ in the spent sample can be calculated as following:

$$X_{\mathrm{Ni@SiO_2}} = X_1 \cdot X_2 \quad (12)$$

So that the accumulated carbon to catalyst fraction in mass can be expressed as:

$$X_{Carbon} = (1/X_{\mathrm{Ni@SiO_2}}) - 1 \quad (13)$$

3. RESULTS AND DISCUSSION

3.1 Morphology, structure, crystal phase, and absorption spectrum of $Ni@SiO_2$ catalyst

The SEM and TEM results of $Ni@SiO_2$ sample were depicted in Fig. 2. From the SEM images, the block was formed by close packing hexagonal structure nanosheets, with a lot of voids between them. Notably, the nanosheets were arranged in order and possessed the same normal direction, instead of random distribution. According to the TEM images, the diagonal length of the thin Ni-nanosheets is in range of 120-150nm. And each Ni-sheet was wrapped by the porous SiO_2 shell, which measured 50 nm thick. From Fig. 1d, the shell of the sheet was measured uniformly 25nm thick at each edge, demonstrated the evenness of the shell.

The XRD pattern of $Ni@SiO_2$ was showed in Fig. 3a, which fitted well with the standard crystal information of metallic Ni. Besides, due to the amorphous structure of SiO_2, there were no peaks of silicon oxide detected. From the adsorption spectra in Fig. 3b, the $Ni@SiO_2$ sample showed excellent adsorption in the spectra range of 200-2000 nm.

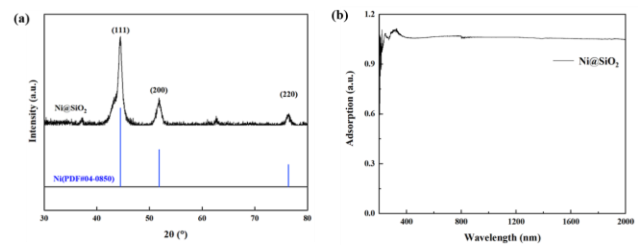

Fig. 3 (a) XRD and (b) the UV-Vis-NIR adsorption spectra of fresh $Ni@SiO_2$.

3.2 Reaction performances of $Ni@SiO_2$ under illumination and in darkness

To investigate the characteristics of light-driven DRM of Ni@SiO2, the catalyst performance was tested under light and in the dark at the temperate range of 400-500 °C, respectively. The light reaction only used a 300 W Xe lamp as the light and energy source without electric heating block. As mentioned above, in order to measure the temperature of the light-driven reaction more accurately, a thermocouple was placed to touch the sample surface from below (Fig. 1a) to control the reaction temperature. As compared in Fig. 4a-b, the light-driven DRM showed superior performance at each temperature point.

At low temperature (400 °C) in the dark, the reaction activity was extremely low and the ratio of H_2/CO was close to 1, meant there was almost no side reaction occurred. With reaction temperature rising, dark reactivity significantly increased and the H_2/CO ratio reduced. Due to the endothermic reaction RWGS was also promoted at high temperature, more inlet CO_2 was consumed by produced H_2. Thus, the CO_2 conversion increased faster along with temperature than CH_4, also, the H2 production rate was lower than CO.

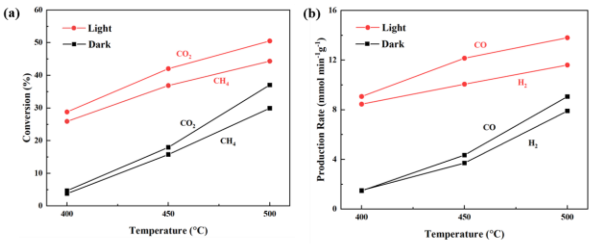

Fig.4 The (a) conversions and (b) production rate of DRM at various temperatures on Ni@SiO$_2$ under illumination and in darkness.

The light reaction owned higher conversions and products, showed that light possessed facilitating effect on the DRM process. Notably, a larger gap between CH_4 and CO_2 was found than the dark reaction, and CO_2 conversion increased faster than CH_4. It meant that more RWGS reaction occurred under focus light. In one aspect, the endothermic reactions DRM and RWGS can be promoted by high temperature, so it is possible that there was some zone at higher temperature than measured. In addition, researchers have found that light has certain activation effect on the chemical bonds so that can activate the reactants and intermediates. Therefore, the species in the reaction got more chance to get higher transient energy and participate in chemical reactions.

From 400 °C to 500 °C, the performance of dark reaction lifted faster than under illumination, indicated that the decline of light-enhancing effect at higher temperature due to the intense driving force from heat. Which implied that light-driven DRM of Ni@SiO$_2$ possessed more advantages at milder temperature. So that medium solar concentration ratio can be combined with DRM, lowered material requirements for the solar reactor. Meanwhile, the severe sintering of catalysts can be mitigated to enhance the material durability.

3.3 Durability and carbon deposition of Ni@SiO2 samples under illumination and in darkness

The long duration catalytic test was lasted for one hour, in which the dark reaction accumulated too much carbon to carry on. As shown in Fig. 5a, the performance of dark reaction decreased after 10 min and the conversion reached a relatively stable activity after 35 min. The higher CO_2 conversion and lower H_2 production rate indicated that RWGS reaction proceeded in the whole duration, which produced CO and H_2O.

The catalyst volume increased obviously during the dark reaction at 500 °C, so that the decline of conversion was led by the carbon accumulation. As the production rate of H_2 maintained stability while CO decreased continuously, the carbon deposition was formed by CH_4 decomposition and possibly from the CO disproportionation.

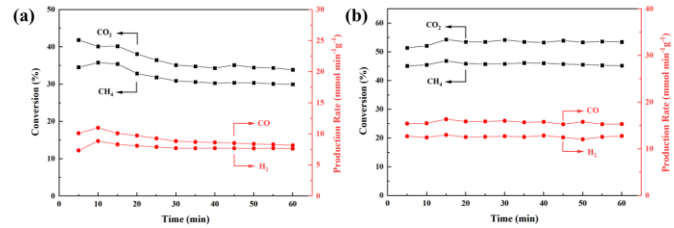

Fig.5 The reaction activity of DRM of Ni@SiO$_2$ (a) in the dark and (b) under light versus reaction time at 500 °C.

For the light reaction, see in Fig. 5b, the slight increase in the initial stage could be caused by the adsorption procedure. Reaching the equilibrium between adsorption and desorption, the performance stabilized within 10 min and remained stable, without obvious sample volume expansion observed. Comparing with dark reaction, the values of CO_2 and CH_4 conversion and the gap between them were all higher under light, meant the solar illumination promoted the DRM and RWGS reactions at the same time.

TGA (Thermogravimetric Analysis) test was adapted to analyze the amount of carbon deposition of Ni@SiO$_2$ samples used under illumination and in darkness. First, the used samples were heated to 600 at air flow (30 mL/min), see in Fig. 6a. After oxidation, the atmosphere was switched to H_2 (H_2 at 10 mL/min with Ar at 20 mL/min) for reducing the NiO, with temperature maintaining (Fig. 6b). The weight of used samples slightly increased during the temperature program oxidation, which was caused by the oxidation of metallic nickel. Then the carbon was oxidized and the weight decreased, and there was only NiO@SiO$_2$ left after the weight loss line stabilized. The fully oxidized sample was then reduced by H_2 to calculate the actual weight of carbon.

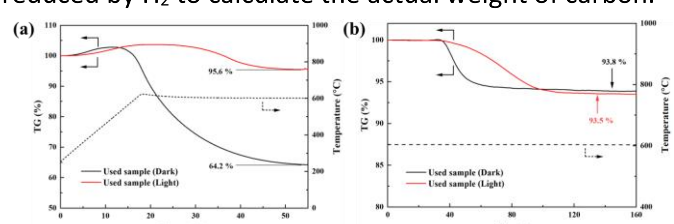

Fig.6 The weight loss profiles of the used samples of Ni@SiO$_2$ in the dark and under light. (a) Oxidation at air flow and (b) reduction in H$_2$.

According to the calculated results, light reaction produced much less carbon (0.12g/h/g$_{catalyst}$) than in darkness (0.66 g/h/g$_{catalyst}$), corresponding to the durability of reaction performance. Which demonstrated that focus light possessed the ability of inhibiting carbon deposition or promoting the oxidation of carbon. Besides, the approximate weight decrease in the reduction certificated the consistency of the samples.

3.4 Mechanism investigation in light-driven DRM of Ni@SiO2

To investigate the mechanism in the reaction process of $Ni@SiO_2$ in photothermal and thermal catalysis, time-resolved *in-situ* diffuse reflectance Infrared Fourier transform spectroscopy (DRIFTS) test was carried out. The results of DRM at 450 ° C were showed in Fig. 7. The peak at 3015 m^{-1} was consistent with CH_4 and the band at 2342 cm^{-1} was corresponding to CO_2[19]. And the intensity of reactants turned to steady along with adsorption. The signal of CH_4 was relatively weaker than CO_2 in Fig. 7a, implied that more cracking consumed the inlet CH_4.

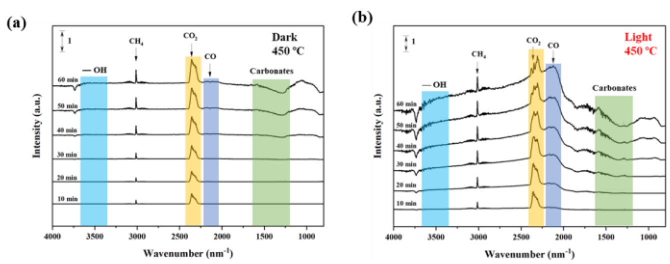

Figure. 7 In-situ DRIFTS spectra of (a) thermal and (b) photothermal DRM of $Ni@SiO_2$.

As there was no dipole moment change of H_2, a completely symmetrical molecule, it showed no infrared activity. Thus, CO was the only signal to present the products, matched the doublet at 2145 cm^{-1}[20]. From Fig. 7b, the CO signal increased faster under illumination, meant higher production rate of light reaction. In addition, the vibration over 3500 cm^{-1} and the band in 1300-1900 cm^{-1} was caused mainly by hydroxy and CH_xO species, respectively[21,22]. The stronger fluctuation in these bands illustrated that the gaseous intermediates were excited at the gas-solid interface by light and gained superior reactivity.

The results from infrared spectrogram were corresponding to the results discussed above, and it can be deduced that focus light facilitated DRM of $Ni@SiO_2$ by activating the intermediates. By contrast, the reaction in darkness was prone to methane cracking, with less reactivity of intermediates.

In conclusion, the main mechanism for light-enhanced performance can be concluded as following:

The local high temperature in the irradiated core-shell sample. The SiO_2 shell of the sample provided a shielding layer to prevent infrared light and heat from dispersing outward, thus, the input light energy was confined in the sheath. Thereby, there was higher temperature in the inside Ni zone. Due to high temperature, the equilibrium of DRM and RWGS reaction shifted positively.

The focus light activated the metallic Ni and chemical bonds of C, H, O species. Ni can be promoted to its excited state with light irradiation and get superior reactivity. Although the E_a values of dissociation of CO_2, CH_4, CH_3 and CH_2 reduces negligibly in the excited state, the oxidation E_a values of C and CH reduce obviously[23]. Thus, the light excitation of species results in the high activity of the DRM reaction.

4. CONCLUSIONS

In summary, a core-shell structured $Ni@SiO_2$ nanosheet was used for thermal and photothermal DRM to investigate the enhancing-effect of focus solar light. The light-driven DRM presented impressive production rates of H_2 and CO (11.6 and 13.8 mmol/min/g, respectively) under 10.6 W/cm^2 full-spectra illumination, higher than the dark reaction (7.9 and 9.1 mmol/min/g for H_2 and CO) at 500 °C. Accordingly, the heat insulation and infrared shielding effects of the SiO_2 shell were demonstrated, which needed further study for its optimal operating temperature in larger range of solar concentration ratio. Also, the photo-enhanced reaction efficiently inhibited carbon deposition during long duration operation. Carbon accumulated in one hour with light was only 18 % of which in darkness, consisted with the DRM durability difference. In addition, the mechanism of photoactivated reactivity was revealed by the *in-situ* DRIFTS study. In the spectroscopy results, the intermediates showed significant activity under irradiation, and thus the light-driven reaction presented superior production rate. Our work investigated the performance and mechanism of photo-enhanced DRM of $Ni@SiO_2$ at mild-temperature, and proved a method of catalyst design for renewable solar energy conversion and CO_2 emission reduction.

ACKNOWLEDGEMENT

The authors would like to acknowledge the support by National Natural Science Foundation of China (NSFC) grant (No. 51888103 and No.52176026).

DECLARATION OF INTEREST STATEMENT

The authors declare that they have no known competing financial interests or personal relationships that could have appeared to influence the work reported in this paper. All authors read and approved the final manuscript.

REFERENCE

[1] Bu K, Kuboon S, Deng J, Li H, Yan T, Chen G, et al. Methane dry reforming over boron nitride interface-confined and LDHs-derived Ni catalysts. Appl Catal B Environ 2019;252:86–97.

[2] Hussien AGS, Polychronopoulou K. A Review on the Different Aspects and Challenges of the Dry Reforming of Methane (DRM) Reaction. Nanomaterials 2022;12.

[3] Rego de Vasconcelos B, Pham Minh D, Sharrock P, Nzihou A. Regeneration study of Ni/hydroxyapatite spent catalyst from dry reforming. Catal Today 2018;310:107–15.

[4] Li Z, Lin Q, Li M, Cao J, Liu F, Pan H, et al. Recent advances in process and catalyst for CO2 reforming of methane. Renew Sustain Energy Rev 2020;134:110312.

[5] Han B, Wei W, Chang L, Cheng P, Hu YH. Efficient Visible Light Photocatalytic CO2 Reforming of CH4. ACS Catal 2016;6:494–7.

[6] Xie Z, Yan B, Lee JH, Wu Q, Li X, Zhao B, et al. Effects of oxide supports on the CO2 reforming of ethane over Pt-Ni bimetallic catalysts. Appl Catal B Environ 2019;245:376–88.

[7] Arora S, Prasad R. An overview on dry reforming of methane: Strategies to reduce carbonaceous deactivation of catalysts. RSC Adv 2016;6:108668–88.

[8] Kim WY, Jang JS, Ra EC, Kim KY, Kim EH, Lee JS. Reduced perovskite LaNiO3 catalysts modified with Co and Mn for low coke formation in dry reforming of methane. Appl Catal A Gen 2019;575:198–203.

[9] Yu M, Zhu YA, Lu Y, Tong G, Zhu K, Zhou X. The promoting role of Ag in Ni-CeO2 catalyzed CH4-CO2 dry reforming reaction. Appl Catal B Environ 2015;165:43–56.

[10] Sun Y, Ritchie T, Hla SS, McEvoy S, Stein W, Edwards JH. Thermodynamic analysis of mixed and dry reforming of methane for solar thermal applications. J Nat Gas Chem 2011;20:568–76.

[11] Rabelo-Neto RC, Sales HBE, Inocêncio CVM, Varga E, Oszko A, Erdohelyi A, et al. CO2 reforming of methane over supported LaNiO3 perovskite-type oxides. Appl Catal B Environ 2018;221:349–61.

[12] Fang X, Zhang J, Liu J, Wang C, Huang Q, Xu X, et al. Methane dry reforming over Ni/Mg-Al-O: On the significant promotional effects of rare earth Ce and Nd metal oxides. J CO2 Util 2018;25:242–53.

[13] Mourhly A, Kacimi M, Halim M, Arsalane S. New low cost mesoporous silica (MSN) as a promising support of Ni-catalysts for high-hydrogen generation via dry reforming of methane (DRM). Int J Hydrogen Energy 2020;45:11449–59.

[14] Huang F, Wang R, Yang C, Driss H, Chu W, Zhang H. Catalytic performances of Ni/mesoporous SiO2 catalysts for dry reforming of methane to hydrogen. J Energy Chem 2016;25:709–19.

[15] Zhang Q, Zhang T, Shi Y, Zhao B, Wang M, Liu Q, et al. A sintering and carbon-resistant Ni-SBA-15 catalyst prepared by solid-state grinding method for dry reforming of methane. J CO2 Util 2017;17:10–9.

[16] Lovell E, Jiang Y, Scott J, Wang F, Suhardja Y, Chen M, et al. CO2 reforming of methane over MCM-41-supported nickel catalysts: altering support acidity by one-pot synthesis at room temperature. Appl Catal A Gen 2014;473:51–8.

[17] Qian L, Huang K, Wang H, Kung MC, Kung HH, Li J, et al. Evaluation of the catalytic surface of Ni impregnated meso-microporous silica KIT-6 in CH4 dry reforming by inverse gas chromatography. Microporous Mesoporous Mater 2017;243:301–10.

[18] Cai M, Wu Z, Li Z, Wang L, Sun W, Tountas AA, et al. Greenhouse-inspired supra-photothermal CO2 catalysis. Nat Energy 2021;6:807–14.

[19] Busca G, Lorenzelli V. Infrared study of CO2 adsorption on haematite. Mater Chem 1980;5:213–23.

[20] Ni J, Chen L, Lin J, Kawi S. Carbon deposition on borated alumina supported nano-sized Ni catalysts for dry reforming of CH4. Nano Energy 2012;1:674–86.

[21] Karelovic A, Ruiz P. Improving the Hydrogenation Function of Pd/γ-Al2O3 Catalyst by Rh/γ-Al2O3 Addition in CO2 Methanation at Low Temperature. ACS Catal 2013;3:2799–812.

[22] Cárdenas-Arenas A, Quindimil A, Davó-Quiñonero A, Bailón-García E, Lozano-Castelló D, De-La-Torre U, et al. Isotopic and in situ DRIFTS study of the CO2 methanation mechanism using Ni/CeO2 and Ni/Al2O3 catalysts. Appl Catal B Environ 2020;265:118538.

[23] Mao M, Zhang Q, Yang Y, Li Y, Huang H, Jiang Z, et al. Solar-light-driven CO2 reduction by methane on Pt nanocrystals partially embedded in mesoporous CeO2 nanorods with high light-to-fuel efficiency. Green Chem 2018;20:2857–69.